Peregrine soliton generation and breakup in standard telecommunications fiber

Kamal Hammani,[1] Bertrand Kibler,[1,*] Christophe Finot,[1] Philippe Morin,[1] Julien Fatome,[1] John M. Dudley,[2] and Guy Millot[1]

[1]*Laboratoire Interdisciplinaire Carnot de Bourgogne, UMR 5209 CNRS/Université de Bourgogne, 21078 Dijon, France*

[2]*Institut Femto-ST, UMR 6174 CNRS/Université de Franche-Comté, 25030 Besançon, France*

**Corresponding author: bertrand.kibler@u-bourgogne.fr*

Received October 29, 2010; accepted November 22, 2010;
posted December 6, 2010 (Doc. ID 137339); published January 5, 2011

We present experimental and numerical results showing the generation and breakup of the Peregrine soliton in standard telecommunications fiber. The impact of nonideal initial conditions is studied through direct cutback measurements of the longitudinal evolution of the emerging soliton dynamics and is shown to be associated with the splitting of the Peregrine soliton into two subpulses, with each subpulse itself exhibiting Peregrine soliton characteristics. Experimental results are in good agreement with simulations. © 2011 Optical Society of America

OCIS codes: 060.4370, 060.5530.

There is currently much research interest in extreme value fluctuations and "optical rogue wave" localization processes in nonlinear fiber optics and supercontinuum generation [1,2]. These results have motivated a number of studies into the initial dynamics of the supercontinuum generation process, and it was shown in particular that the temporal and spectral characteristics of the evolving field could be well described in terms of a particular class of nonlinear Akhmediev breather (AB) structure that undergoes periodic evolution with propagation and periodic energy exchange with a finite background [3]. AB characteristics are observed when a weakly modulated cw is injected in the anomalous dispersion regime of an optical fiber, and can be described in terms of an analytic solution of the nonlinear Schrodinger equation (NLSE) given by [4–6]

$$A(z,T)=\sqrt{P_0}\,\frac{(1-4a)\cosh(bz/L_{\mathrm{NL}})+ib\sinh(bz/L_{\mathrm{NL}})+\sqrt{2a}\cos(\omega_{\mathrm{mod}}T)}{\sqrt{2a}\cos(\omega_{\mathrm{mod}}T)-\cosh(bz/L_{\mathrm{NL}})}. \tag{1}$$

Here, $A(z,T)$ is the field envelope, and the injected field has average power P_0 and is modulated at frequency ω_{mod}. Breather dynamics are observed for frequencies experiencing modulation instability gain, corresponding to $0<a<1/2$ with $2a=[1-(\omega_{\mathrm{mod}}/\omega_c)^2]$ and $\omega_c^2=4\gamma P_0/|\beta_2|$. Here, γ and β_2 refer to the fiber nonlinearity and dispersion, the nonlinear length is $L_{\mathrm{NL}}=(\gamma P_0)^{-1}$, and the parameter $b=[8a(1-2a)]^{1/2}$ determines the instability growth. The asymptotic case $a\to 1/2$ is known as the Peregrine soliton (PS) and is of particular interest, as it represents the analytical limit of a wide class of NLSE solutions and because it has the rational form $A(z,T)=\sqrt{P_0}[1-4(1+2iz/L_{\mathrm{NL}})/(1+4(T/T_0)^2+4(z/L_{\mathrm{NL}})^2]\exp(iz/L_{\mathrm{NL}})$, where $T_0=(\beta_2 L_{\mathrm{NL}})^{1/2}$.

Despite its existence in the mathematical literature for over 25 years, the PS solution has only very recently been observed in experiments. Two narrow-linewidth lasers were used to generate initial conditions to excite PS localization in highly nonlinear fiber, characterized using intensity and phase measurements with frequency-resolved optical gating [7].

In this Letter, we further explore the generation of PS characteristics in fibers, using a much simplified setup that allows us to study the evolution dynamics over a wider range of initial conditions. The setup is shown in Fig. 1 and is based exclusively on commercially available telecommunication-ready components and standard silica SMF-28 fiber. In contrast to previous experiments using combined external cavity lasers to create an amplitude modulated beat signal, we use a simpler approach here, with a directly intensity modulated 1550 nm laser diode and an ultrafast optical sampling oscilloscope (OSO—Picosolve PSO100 series) that enables real-time observation of the temporal reshaping toward the PS. We also perform high-dynamic-range spectral characterization, and note that a phase modulator is used to prevent from the deleterious consequences of Brillouin scattering, and an erbium-doped fiber amplifier (EDFA) is used to obtain average powers up to 1 W. The optical fiber is an 8.35-km-long segment of SMF-28 with $\beta_2=-21.4$ ps^2/km, $\beta_3=0.12$ ps^3/km,

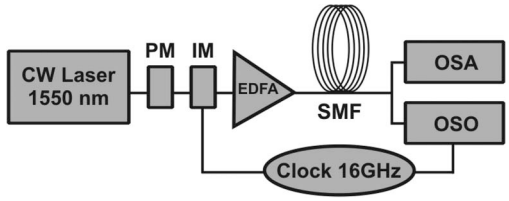

Fig. 1. (Color online) Experimental setup. PM, phase modulator; IM, intensity modulator; OSO, optical sampling oscilloscope; OSA, optical spectrum analyzer.

$\gamma = 1.2\ \mathrm{W^{-1}\cdot km^{-1}}$, and 0.19 dB/km loss. The output signal is carefully characterized both in the temporal and spectral domains by means of an OSA and an OSO that enables the direct measurement of the (subpicosecond) intensity profile in real time. By combining the real-time characterization with cutback measurements, we provide what we believe to be the first direct observation of PS longitudinal evolution dynamics and report an effect associated with the breakup of a PS into two subpulses, each possessing similar characteristics of localization upon finite background.

The field injected into the fiber is $A(z=0,T) = \sqrt{P_0}[1+\delta_{\mathrm{mod}}\cos(\omega_{\mathrm{mod}}T)]^{1/2}$, where δ_{mod} is the intensity modulation contrast. As this modulated field propagates along the fiber, it undergoes dynamical nonlinear compression to yield pulses that grow to high amplitude before returning to the initial state through Fermi–Pasta–Ulam (FPU) recurrence. Our present setup is very convenient for studying the precise impact of the initial conditions on this evolution. Indeed, we performed temporal and spectral characterization at $\omega_{\mathrm{mod}}/2\pi = 16$ GHz using different values of δ_{mod} in the range 0.2–0.6 and 12 values of power P_0 from 0.35 to 0.9 W. The power range, in particular, enables us to study the dynamics over an extended region of the gain curve from $0.4 < a < 0.47$, allowing us to approach the ideal PS limit much more closely than in previous experiments performed at $a = 0.42$ [7]. Moreover, the longitudinal evolution of the field was studied by cutting the fiber in 32 parts.

The first results we present inFig. 2 concern the propagation dynamics as a function of power and distance.

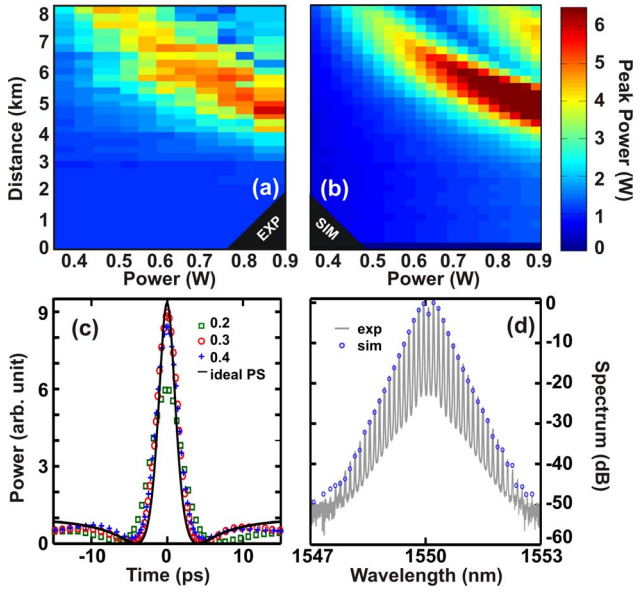

Fig. 2. (Color online) False-color maps showing compressed peak power as a function of distance and power at $\delta_{\mathrm{mod}} = 0.3$ from: (a) experiment and (b) simulation. (c) Comparison of the temporal intensity profile measured for three values of δ_{mod} at corresponding optimum compression distance with $P_0 = 0.8$ W (see details in the text). The ideal analytic PS is also shown in the black curve. Corresponding numerical simulations of $\delta_{\mathrm{mod}} = 0.3$ yield results that are indistinguishable from the experimental data. (d) Corresponding spectrum (solid curve) at maximum compression for $\delta_{\mathrm{mod}} = 0.3$ compared with numerical results (open circles).

At fixed modulation contrast $\delta_{\mathrm{mod}} = 0.3$, Fig. 2(a) illustrates how the degree of dynamical compression strongly depends on initial conditions by plotting the compressed pulse peak power as a function of propagation distance for powers in the range 0.35–0.9 W. The peak power was determined from average power measurements and the measured OSO temporal profiles. The results are shown in false-color representation, clearly illustrating how the distance of optimum compression decreases at higher powers. The experimental results are compared with numerical simulations shown in Fig. 2(b). At the highest powers, the simulations also show the appearance of a secondary compression phase; we study this feature in more detail in Fig. 3, where we show that it is associated with a pulse-splitting effect.

The PS propagation dynamics are known to depend sensitively on the initial modulation depth. Indeed, the ideal evolution toward the PS is expected to occur for smaller values of δ_{mod} with evolution over a longer propagation distance [3]. For fixed input power $P_0 = 0.80$ W, Fig. 2(c) presents results for three values of $\delta_{\mathrm{mod}} = 0.2$, 0.3, 0.4, where we plot the temporal intensity profile measured at the distance of optimum compression $L = 7.3$, 4.6, 4.2 km, respectively. We clearly see that lower δ_{mod} requires longer propagation distances for optimal compression, but our ability to readily characterize the evolution for these different cases allows us to see that greater propagation distance associated with the lowest δ_{mod} results in deviation from the ideal PS characteristics

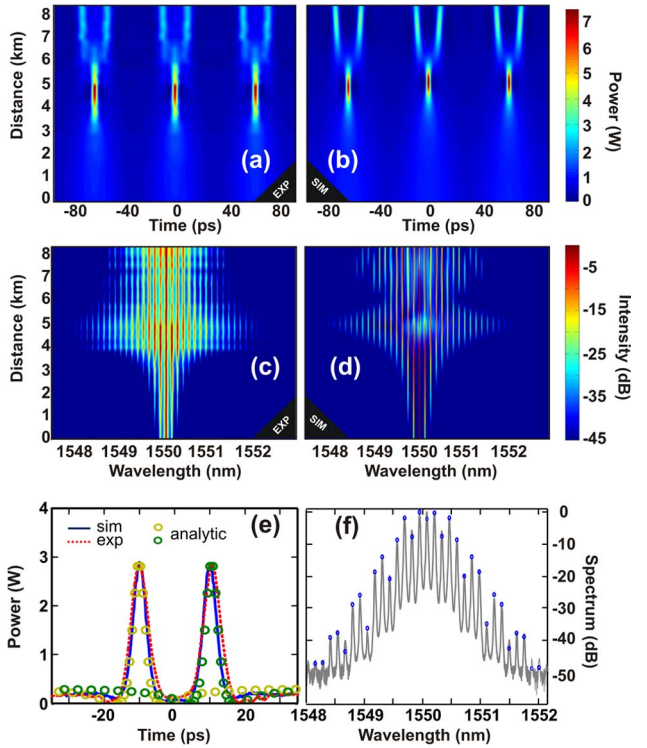

Fig. 3. (Color online) Evolution with distance of (a), (b) temporal and (c), (d) spectral intensities comparing experiment and simulation as shown. Here $\delta_{\mathrm{mod}} = 0.3$ and $P_0 = 0.80$ W. (e) OSO signal observed at 8.4 km with $\delta_{\mathrm{mod}} = 0.3$. Experiment (dashed curve) is compared with simulations (solid curve) and the analytical form of PS for each subpulse (open circles). (f) Corresponding spectrum with solid curve compared with numerical spectrum (open circles).

because of significant loss. From our results, the best agreement with the expected PS structure is at $\delta_{\mathrm{mod}} = 0.3$, where we see a clear temporally localized peak surrounded by a nonzero background. The central part of the structure has a temporal duration around 3 ps and closely follows the analytical formula as well as the numerical simulations based on the extended NLSE taking into account third-order dispersion, losses, Raman effects, and ASE noise at the experimental level. The excellent agreement observed in the temporal domain is also confirmed in the spectral domain, as illustrated in Fig. 2(d).

We now focus in more detail on the whole longitudinal evolution of the field corresponding to the results in Figs. 2(c) and 2(d) when $\delta_{\mathrm{mod}} = 0.3$ and $P_0 = 0.8$ W (i.e., $a = 0.47$). Figure 3 shows the longitudinal evolution of the temporal and spectral profiles obtained from experiment [(a), (c)] and numerical simulations [(b), (d)]. We clearly observe the temporal evolution of themodulated cw field into a periodic train of ultrashort pulses on a continuous background, accompanied by a significant spectral broadening. Experiments and simulations are in excellent agreement but significantly differ after the point of optimal compression. We do not observe the expected return to the initial state but rather a striking effect of Peregrine soliton breakup into two identical structures. Corresponding temporal and spectral signatures of these dynamics can also be seen in Figs. 3(e) and 3(f).

The deviation from recurrent dynamics is attributed to the sensitivity of the propagation to nonideal initial conditions as we approach the PS limit at higher values of a [4]. We stress that this behavior was not observed in previous experiments where lower values of a and more restricted propagation were used [7], and thus these results represent a significant observation. In fact, our ability to readily characterize the temporal profiles using the OSO allows us to further see that the subpulses are each themselves very well fitted by the analytical form of the ideal PS; comparison with the ideal PS for each subpulse is shown in Fig. 3(e), using $P_0 = 0.32$ W equal to the continuous background around the doublet pulses. This suggests that the Peregrine soliton profile represents an attractive structure after breakup processes, similar to behavior of the more well-known hyperbolic secant solitons of the NLSE. However, further theoretical work will be needed to determine the precise conditions under which such breakup is initiated [8]. In particular, a recent study has reported specific conditions for which FPU recurrence can be affected by frequency-doubling dynamics [9].

There are several conclusions to be drawn from this work. First, we have shown that it is possible to generate near-ideal Peregrine soliton localization and to characterize the associated dynamics using a simple experimental setup with standard telecommunications components and measurement techniques. This allows the evolution of an initially modulated field toward the Peregrine soliton to be studied in a parameter limit very closely approaching the ideal theoretical limit and also permits the convenient and direct characterization of the propagation dynamics through cutback measurements. These experiments reveal new features of this class of two-dimensional localization dynamics, including the sensitivity of the optimally compressed profile on modulation depth, as well as a phenomenon of pulse breakup, as the expected FPU recurrence is not observed with our experimental parameters. We anticipate that these results will impact on studies of the emergence of extreme localized events in optics under various initial excitation conditions. In a wider context, the fact that an initial Peregrine soliton can break up into two lower amplitude but equally strongly localized soliton pulses may have important implications for further interpretations of hydrodynamic rogue wave observations [10].

This work was supported by the Agence Nationale de la Recherche (ANR MANUREVA project ANR-08-SYSC-019) and by the Conseil Régional de Bourgogne.

References

1. D. R. Solli, C. Ropers, P. Koonath, and B. Jalali, Nature **450**, 1054 (2007).
2. J. M. Dudley, C. Finot, G. Millot, J. Garnier, G. Genty, D. Agafontsev, and F. Dias, Eur. J. Phys. Spec. Top. **185**, 125 (2010).
3. J. M. Dudley, G. Genty, F. Dias, B. Kibler, and N. Akhmediev, Opt. Express **17**, 21497 (2009).
4. N. Akhmediev and V. I. Korneev, Theor. Math. Phys. **69**, 1089 (1986).
5. K. B. Dysthe and K. Trulsen, Phys. Scripta **T82**, 48 (1999).
6. N. Akhmediev, A. Ankiewicz, and M. Taki, Phys. Lett. A **373**, 675 (2009).
7. B. Kibler, J. Fatome, C. Finot, G. Millot, F. Dias, G. Genty, N. Akhmediev, and J. M. Dudley, Nat. Phys. **6**, 790 (2010).
8. Y. Kodama and A. Hasegawa, IEEE J. Quantum Electron. **23**, 510 (1987).
9. S. Wabnitz and N. Akhmediev, Opt. Commun. **283**, 1152 (2010).
10. V. I. Shrira and V. V. Geogjaev, J. Eng. Math. **67**, 11 (2009).